

# SCIENTIFIC REPORTS



OPEN

## Podocyte injury in diabetic nephropathy: implications of angiotensin II – dependent activation of TRPC channels

Received: 15 September 2015

Accepted: 03 November 2015

Published: 10 December 2015

Daria V. Ilatovskaya<sup>1</sup>, Vladislav Levchenko<sup>1</sup>, Andrea Lowing<sup>1</sup>, Leonid S. Shuyskiy<sup>1,3</sup>, Oleg Palygin<sup>1</sup> & Alexander Staruschenko<sup>1,2</sup>

Injury to podocytes is considered a major contributor to diabetic kidney disease: their loss causes proteinuria and progressive glomerulosclerosis. Podocyte depletion may result from improper calcium handling due to abnormal activation of the calcium permeant TRPC (Transient Receptor Potential Canonical) channels. Angiotensin II (Ang II) levels are found to be elevated in diabetes; furthermore, it was reported that Ang II causes activation of TRPC6 in podocytes. We hypothesized here that Ang II-mediated calcium influx is aggravated in the podocytes under the conditions of type 1 diabetic nephropathy (DN). Diabetes was induced in the Dahl Salt-Sensitive rats by an injection of streptozotocin (STZ-SS). Eleven weeks post treatment was sufficient for the animals to develop hyperglycemia, excessive urination, weight loss, microalbuminuria, nephrinuria and display renal histological lesions typical for patients with DN. Patch-clamp electrophysiology performed on podocytes of the freshly isolated glomeruli showed enhanced basal TRPC channel activity in the STZ-SS rats, and increased response to Ang II; total calcium influx triggered by Ang II application was also augmented in podocytes of these rats. Our studies have a strong potential for advancing the understanding of TRPC-mediated effects on podocytopenia in DN initiation.

Currently about 347 million people are suffering from diabetes mellitus, and recent estimates put more than 439 million adults worldwide in danger of diabetes and its complications by 2030<sup>1</sup>. Diabetic nephropathy (DN) is among the most serious complications of both type 1 and type 2 diabetes, and often leads to end-stage renal disease ultimately requiring renal transplantation. The characteristic pathological changes of DN include severe albuminuria, renal hyperfiltration, glomerular basement membrane thickening, and glomerulosclerosis<sup>2</sup>. In the early onset of DN a dramatic decrease in the podocyte number is observed (even before the manifestation of albuminuria<sup>3</sup>), which results in the loss of the filtration barrier integrity, and consequent pathological changes in glomeruli permeability<sup>4,5</sup>. Podocytes are highly specialized epithelial cells located on the surface of the glomeruli capillaries, and normally prevent leakage of protein into the urine<sup>6,7</sup>. Since these cells are unable to divide, their injury and malfunction leads to proteinuria, accumulation of extracellular matrical components, and glomerulosclerosis. Additionally, podocyte depletion and structural changes are suggested to be predictors of DN progression<sup>8,9</sup>.

The mechanisms that underlie podocyte apoptosis are a focus of intense research. A novel promising target was revealed in this area several years ago: the TRPC6 (Transient Receptor Potential Canonical) calcium channel. Accumulating evidence suggested that TRPC6 channels are crucial mediators of podocyte calcium handling, and are involved in mediating glomerular permeability and maintaining the renal filtration barrier<sup>10,11</sup>. TRPC6 channels are recognized among the emerging determinants of podocyte injury. The compelling evidence supporting this view was presented when a gain-of-function mutation in TRPC6, which leads to the development of the Focal Segmental Glomerulosclerosis (FSGS), was discovered<sup>12</sup>. Enhanced TRPC6 expression, specifically in the podocytes, led to glomerular damage<sup>10,13</sup>. It is of particular interest that increased expression of the native TRPC6 was

<sup>1</sup>Department of Physiology, Medical College of Wisconsin, Milwaukee, Wisconsin 53226, USA. <sup>2</sup>Cardiovascular Center, Medical College of Wisconsin, Milwaukee, Wisconsin 53226, USA. <sup>3</sup>Institute of Cytology, Russian Academy of Sciences, St. Petersburg, Russian Federation. Correspondence and requests for materials should be addressed to A.S. (email: staruschenko@mcw.edu)

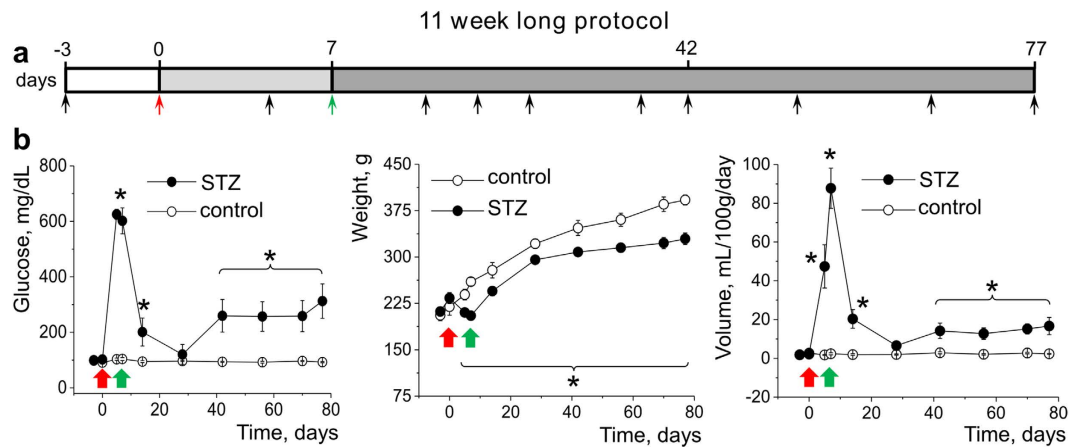


**Figure 1. Development of STZ-induced diabetic nephropathy in Dahl SS rats during the 11 week long protocol.** (a) Experimental protocol used for type 1 diabetes induction in the Dahl SS rat. (b) Development of diabetes in SS rats during 11 weeks after STZ injection as monitored by blood glucose level, body weight and urine output changes. The red and green arrows denote the time of STZ injection and subsequent insulin pellet implantation, respectively. N = 8 rats in control and 9 rats in the STZ-SS group. Asterisk denotes statistically significant difference from control values ( $p < 0.05$ ).

found in the podocytes of patients and animals with proteinuric kidney disease<sup>13,14</sup>. Therefore, it was suggested that TRPC6 causes podocyte injury via up-regulation of calcium flux which ultimately results in apoptosis<sup>15,16</sup>.

Currently, therapeutic targeting of the renin-angiotensin system (RAS) is the most validated clinical strategy for slowing the progression of DN. Ang II released into the renal interstitium is one of the key mediators of renal inflammation and fibrosis in progressive chronic nephropathies. High intrarenal Ang II levels have been definitively linked to glomeruli damage in DN<sup>2,43–46</sup>, whereas the fundamental effector of Ang II in the podocytes remained to be determined. TRPC channels have been associated with Ang II-induced calcium influx in many renal cell types<sup>17–21</sup>. Convincing studies reported that Ang II can aggravate albuminuria by activating TRPC6 channels in podocytes<sup>22</sup>, and Ang II - induced podocyte apoptosis involves altered TRPC6 expression and  $Ca^{2+}$  influx<sup>23</sup>. In our recent publications using knockout animal models we demonstrated the Ang II - dependent up regulation of TRPC6 channels in the podocytes of freshly isolated glomeruli at the level of single ion channel activity<sup>20</sup>. Our data revealed that the TRPC6 channel is responsible for the acute Ang II-activated calcium influx in the podocytes.

The current study tests the long-term effects of Ang II on TRPC6 channels in a model of type 1 diabetes induced in Dahl SS rats with a single injection of STZ (further referred to as STZ-SS)<sup>24</sup>. Slaughter *et al.* conducted a comprehensive analytical study and provided evidence that STZ-SS rats develop hyperfiltration, progressive proteinuria, and display renal histological lesions characteristic of those seen in patients with DN, as distinct from salt resistant Sprague Dawley or other rodent models, which have hyperglycemia, but lack essential DN features<sup>24</sup>. We hypothesized here that Ang II-mediated calcium influx can be aggravated in the DN podocytes, which could further lead to podocytopenia and subsequent proteinuria. The STZ-SS model in combination with unique electrophysiological approaches allowed us to measure single TRPC channel activity and live calcium concentration changes in the podocytes of the freshly isolated glomeruli. Also, for the first time we demonstrated the enhanced TRPC-mediated calcium influx in response to Ang II in the podocytes undergoing DN-related pathological changes.

## Results

### Development of diabetic nephropathy in Dahl SS rats 6 and 11 weeks after an injection of STZ.

Induction of diabetes in Dahl SS rats (6 week old) was performed with an *i.p.* injection of streptozotocin (STZ). After hyperglycemia was confirmed (on day 5 after the injection), an insulin pellet was implanted *s.c.* and the animals were continuously monitored for 6 or 11 weeks. Fig. 1a and Supplementary Fig. 1a demonstrate the schematic representations of the 6 and 11 week long experimental protocols, featuring the days of injection, pellet implantation, and time points when urine samples were taken and blood sugar was measured. During both the 6 and 11 week protocols an initial period of severe hyperglycemia was observed within a week after the injection (up to 600 mg/mL compared to 90 mg/mL in a control group), followed by a reduction in glucose levels as a result of the insulin pellet implantation (see Fig. 1b and Supplementary Fig. 1b). Disease progression was reflected by severe polyuria and a significant decrease in the body weight of the STZ-treated rats when compared to vehicle treated rats. However, as evident from the graphs shown in Fig. 1b and Supplementary Fig. 1b, an 11 week long protocol revealed a more sustained difference in blood sugar, body weight and urine volume between the two groups. These data were confirmed by histological studies and glomeruli scoring. Fig. 2a,b and Supplementary Fig. 1c show representative images of the cortical slices of control and STZ-treated rat kidneys (terminal collection after 6 or 11 week experiments) stained with Masson's trichrome. The 6 week long protocol did not produce kidney damage characteristic of DN (fibrosis, glomerulosclerosis, glomerular basement membrane thickening, etc), whereas 11 weeks of hyperglycemia resulted in significant glomeruli damage (Fig. 2a). To assess the degree of injury, glomeruli were scored on a scale of 0 (healthy glomerulus) to 4 (severe fibrosis and damage). Results summarized

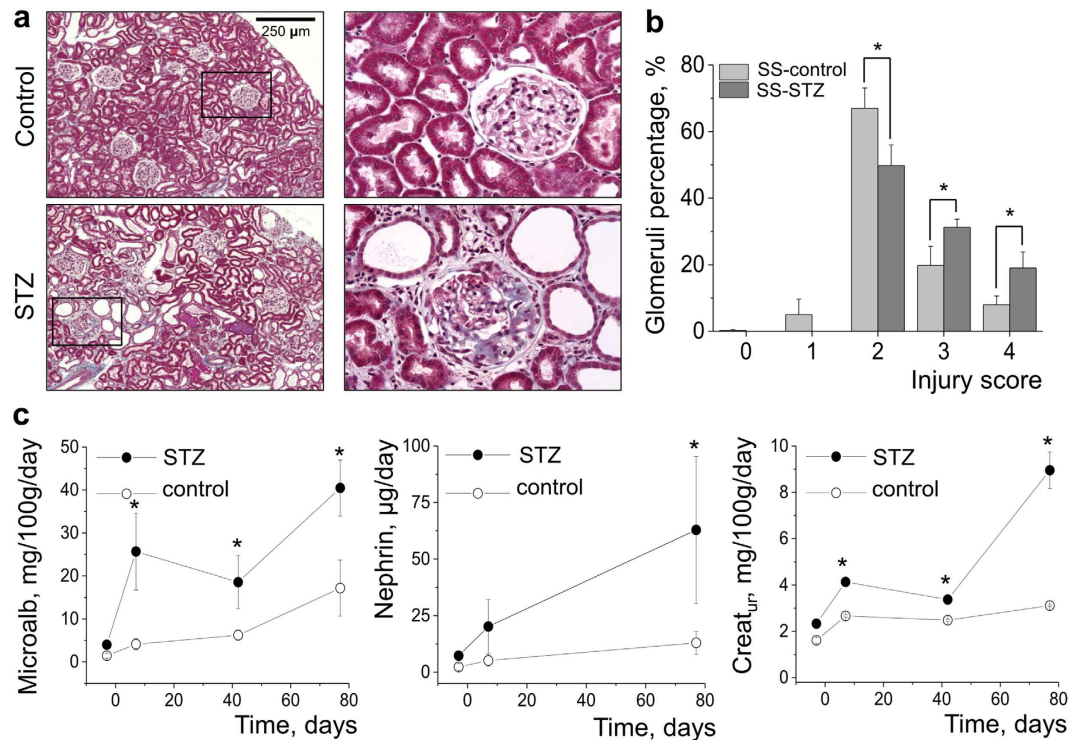


**Figure 2. Kidney injury evaluation, microalbuminuria and nephrinuria in the course of DN development in STZ-treated SS rats.** All measurements were taken during the 11 week long protocol. (a) Histological changes indicative of DN progression in the kidney tissue of STZ-SS rats compared to control animals. Shown are cortical fragments of the trichrome stained kidneys at 10 x and 40 x magnifications. (b) Glomerular injury quantification; at least 4 rats and 100 glomeruli per rat were evaluated in each group. Asterisk denotes difference from the corresponding value in control rats,  $p < 0.05$ . (c) Microalbuminuria, nephrinuria and urinary creatinine in STZ-SS rats versus control animals; urine samples were taken for analysis 3 days before STZ injection, on day 7 after STZ injection (day of implant administration), day 42 (except for nephryn measurement), and day 77 (terminal point). Asterisks located above the data points in the STZ-treated group denote difference from the corresponding value in control group,  $p < 0.05$ .  $N = 8$  rats in control and 9 rats in STZ-injected group.

in Supplementary Fig. 1 demonstrate that 6 weeks of hyperglycemia was not enough to develop glomerular lesions compared to control (although proteinuria was developed – see Supplementary Fig. 1b), whereas an 11 week long protocol (Fig. 2b) caused an increase in the number of severely damaged cortical glomeruli.

Additionally, we tested urinary protein and electrolyte excretion during the time course of diabetes development. As reported in Fig. 2c, a stable increase in urinary microalbumin excretion was observed throughout the experiment in STZ-treated rats compared to the control group, which is indicative of impaired renal function. Furthermore, substantial urinary nephryn shedding was observed in the hyperglycemic animals (measured by an ELISA assay, Fig. 2c, middle graph); detection of nephryn in the urine is considered a solid marker of podocyte injury<sup>25</sup>, therefore, this finding confirms the data acquired by glomeruli scoring. Urinary creatinine levels tested throughout of the experiment (Fig. 2c (right graph)) were found to be significantly elevated in diabetic animals compared to controls, which is indicative of the damaged filtration mechanism. Sodium and potassium excretion rates (Supplementary Fig. 2) were only found to be significantly increased in STZ-treated animals compared to control animals on day 7, which should be attributed to severe polyuria developed by the animals before the insulin pellet was administered. Fractional excretion of sodium and potassium was not altered between the hyperglycemic and control groups at the terminal time point (Supplementary Fig. 2).

### Basal calcium handling is exacerbated in the podocytes during development of diabetic nephropathy.

On day 77 after the STZ injection, animals were sacrificed and tissues were collected for subsequent isolation of glomeruli which were then analyzed. We tested basal calcium concentration levels in the podocytes using ratiometric confocal calcium measurements. Figure 3a shows the representative traces typically used to assess intracellular calcium concentration with the help of ionomycin and  $MnCl_2$ . Calcium levels were recorded as the intensity of Fluo-4,AM calcium binding dye, and obtained data was later recalculated into the intracellular calcium concentration according to the protocol described previously<sup>26</sup>. The summarizing bar graph in Fig. 3b shows a pathologically elevated calcium level in the podocytes of the STZ-treated rats ( $268.3 \pm 30.9$  compared to  $131.1 \pm 8.9$  nM in normoglycemic animals). These data are consistent with the observed increase in basal TRPC channel activity (reported further).

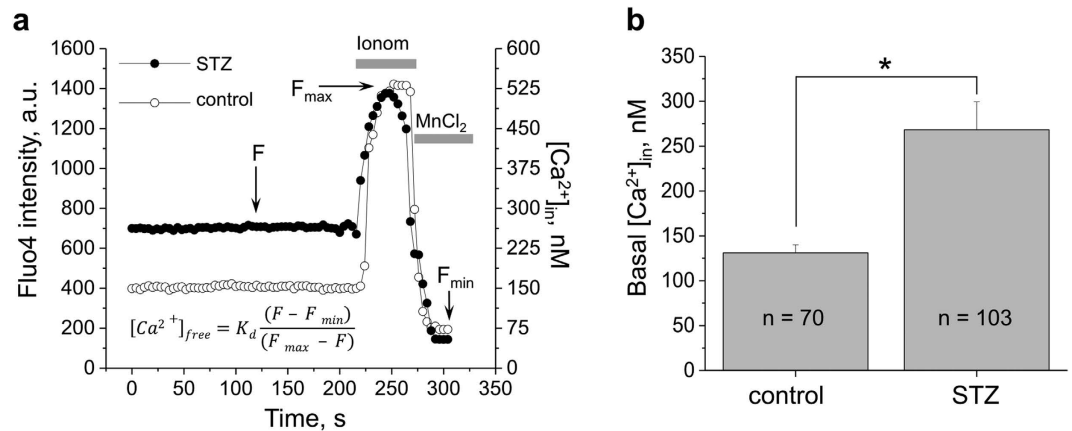


**Figure 3. Basal intracellular calcium concentration is higher in the podocytes of the diabetic animals.** (a) Representative calcium imaging traces showing a typical experiment designed to assess the intracellular calcium level in the podocytes. To measure intracellular calcium concentration, glomeruli were loaded with Fluo-4, AM, fluorescence intensity was recorded in the baseline and after addition of ionomycin and  $\text{MnCl}_2$ . The graph demonstrates the fluorescence signal changes in response to ionomycin (producing the maximum of the Fluo-4, AM fluorescence,  $F_{\max}$ ) and  $\text{MnCl}_2$ , which quenches the dye and results in the lowest fluorescence intensity ( $F_{\min}$ ). Intensity of fluorescence (left axis) for each time point was translated into the actual calcium concentration in nanomoles (right axis) according to the formula shown on the graph. The transients shown on the graph reflect fluorescence intensity of representative ROIs selected from glomeruli of a diabetic and control rat; images were taken every 4 s. (b) Bar graph summarizing the concentration of intracellular calcium in the podocytes of diabetic and control SS rats in the absence of any stimuli. Asterisk denotes statistically significant difference between groups ( $p < 0.05$ ). Number of podocytes analyzed in each group (n) is shown on the graph.

**Diabetic nephropathy is accompanied with up-regulation of calcium influx in response to Ang II in the podocytes of STZ-treated SS rats.** Further pursuing our hypothesis, we questioned whether the increased basal calcium concentration observed in the podocytes of the STZ-treated SS rats (Fig. 3) could be due to the increased calcium influx in response to Ang II. To test this, calcium concentration changes in response to Ang II were measured in freshly isolated glomeruli of control or diabetic SS rats loaded with Fluo-4, AM. Left panel of Fig. 4 reports the typical images of the glomeruli before and after treatment with Ang II (at the peak of the fluorescence intensity). First, it should be noted that the number of podocytes on the surface of the glomeruli of STZ-treated rats was typically decreased (illustrated by the representative images), which is characteristic for the development of DN. Furthermore, Ang II induced a much higher raise in Fluo-4, AM intensity in the podocytes of the diabetic animals compared to vehicle-treated rats. As reported in Fig. 4, we observed an average 1.5 fold increase in Fluo-4, AM intensity upon stimulation with Ang II in the diabetic rat podocytes compared to controls.

**Ang II – dependent stimulation of the TRPC channel activity is enhanced in STZ-treated Dahl SS rats.** As described above, basal calcium concentration and calcium influx in response to Ang II in the podocytes of the diabetic rats was significantly increased compared to the control group. We have shown earlier in our studies that the major part of the Ang II – dependent calcium influx in the podocytes is mediated via TRPC6 calcium channels<sup>20</sup>. To confirm our hypothesis that TRPC channels are also involved in transducing the enhanced Ang II – mediated calcium signaling in DN, we directly tested the activity of TRPC channels in our preparation. First, patch clamp electrophysiology revealed a significant increase in the number of the TRPC channels registered in each patch (from  $1.25 \pm 0.16$  in the podocytes of control rats up to  $1.9 \pm 0.23$  in STZ-treated animals), which aligns with the increased basal calcium levels shown in Fig. 3.

Our previous studies<sup>20</sup> on the wild type and TRPC6 knockout mice revealed that Ang II activated TRPC6 calcium channels in the podocytes. Here, we first confirmed that we are able to register the activity of the TRPC6 channels in rat podocytes. Recorded channels' characteristics were similar to that of the TRPC6 channel we reported earlier in mice<sup>20</sup> - reverse potential close to 0 mV, conductance of  $18.6 \pm 1.7$  pS (data not shown). We have further shown that in the Dahl SS rats TRPC6 channels can be activated by Ang II. Fig. 5a illustrates a typical course of a patch-clamp experiment, where Ang II was applied to the bath solution and caused a fast and robust increase in the TRPC6 open probability, followed by a washout which resulted in a fast decay in the channel's activity.

In our subsequent experiments we tested how the endogenous single TRPC6 channels recorded in the podocytes of the STZ-SS and control rats respond to Ang II. As seen on the current traces obtained with patch-clamp electrophysiology (see Fig. 5b, left panel), we observed a significantly enhanced response to Ang II in the podocytes of the diabetic animals compared to the normoglycemic SS rats. As reported in Fig. 5b (right panel), the increase in open probability of the TRPC6 channels in response to Ang II was substantially higher in the podocytes of the hyperglycemic rats ( $0.29 \pm 0.12$ ) compared to control rats ( $0.6 \pm 0.1$ ). Also, there was a tendency for an increase in basal TRPC6 activity in the podocytes of the diabetic rats; however, it was not significantly different from the control group. Western blotting (Fig. 6a) also demonstrated enhanced expression of TRPC6 proteins ( $1.45 \pm 0.08$  fold) in the isolated kidney cortex of the STZ-SS rats compared to control. Furthermore, the incidence of TRPC6 in



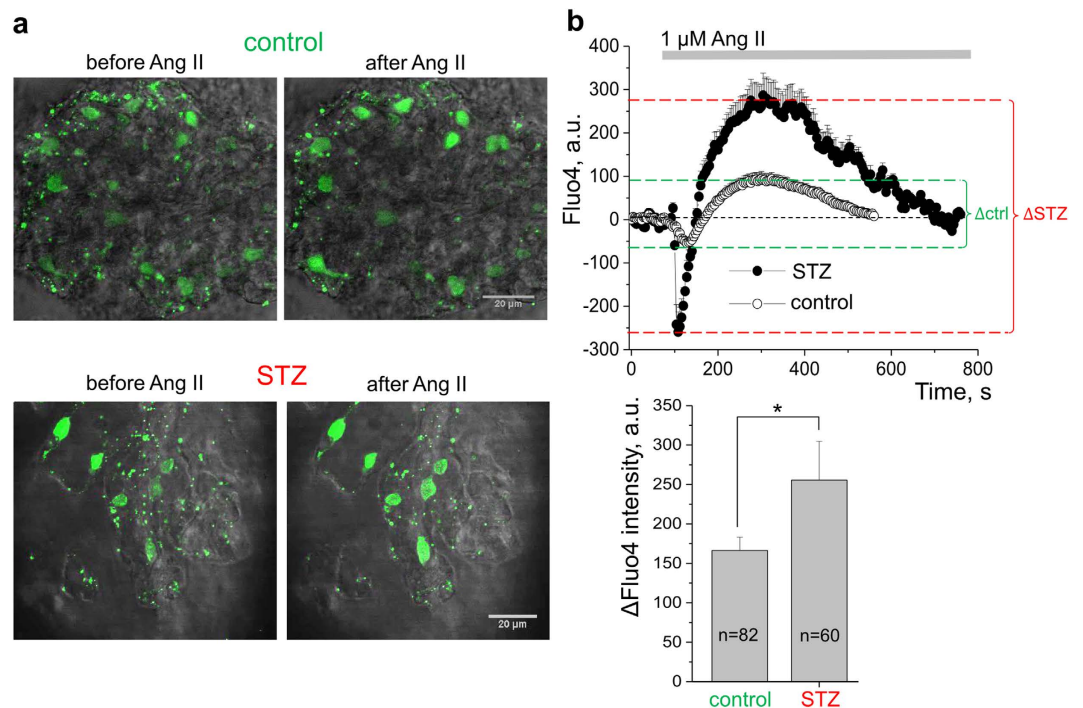


**Figure 4.** Ang II-stimulated calcium influx in the podocytes of STZ-treated and control rats. (a) Representative images of the Fluo-4,AM loaded glomeruli of control (upper row) and diabetic (lower row) SS rats before application of Ang II and at the point of maximal calcium influx after addition of the drug. Fluo-4,AM fluorescence intensity is positively related to calcium concentration within the podocytes. (b) Upper row demonstrates representative transients of intracellular calcium dynamics in the podocytes of the Fluo-4,AM loaded control and STZ-SS rat glomeruli. Lower row shows the bar graph summarizing the relative changes in intracellular calcium concentration in response to Ang II in STZ-treated and control animals (reflected by Fluo-4,AM intensity). Number of podocytes for each group (n) is shown, asterisk indicates  $p < 0.05$ . N of rats used for these measurements was 7 in control and 6 in STZ-injected group.

patches was higher in the podocytes subject to hyperglycemia (45.5% of patches on STZ-treated animals compared to 19.6% in control). Immunohistochemical staining (Fig. 6b) confirmed expression of TRPC6 channels in the podocytes of the glomeruli and cortical tubules of the STZ-treated rats. Furthermore, it appears that expression level of TRPC6 is higher in podocytes of STZ-treated SS rats. However, it is difficult to perform quantification analysis with currently available antibodies.

## Discussion

We report here our recent findings on the role of Ang II – dependent activation of the podocytic TRPC channels in the development of DN. We have utilized the model of DN developed on the basis of Dahl SS rats<sup>24</sup>. The first set of experiments looked at whether 6 and 11 weeks after STZ injection were sufficient for the development of DN. As shown in Figs 1 and 2, the 11 week long treatment resulted in histological and systemic changes characteristic for DN (stable hyperglycemia, weight loss, polyuria, glomerulosclerosis, kidney tissue fibrosis, as well as microalbuminuria and nephrinuria). Basal calcium levels were increased in the podocytes of the STZ-treated rats, and patch-clamp experiments revealed that the chance of registering TRPC6 channel activity was significantly higher in the podocytes of the STZ-treated animals. These results are in accordance with the data reporting increased expression of TRPC6 channels found in the kidney cortex of subjects with acquired glomerular disease<sup>13,14,27</sup>. It should be noted that STZ-SS and control rats were fed a low salt diet (0.4% NaCl), and as shown before by Slaughter *et al.* both groups develop mild hypertension independent of the STZ injection<sup>24</sup>.

Efforts of numerous research groups have recently been focused on the role of glucose in TRPC6 regulation. It was found that in cultured podocytes high glucose induces apoptosis by stimulating TRPC6 via elevation of reactive oxygen species (ROS)<sup>28</sup>, which was later supported by another study demonstrating a glucose-dependent increase in TRPC6 channels expression regulated via oxidative stress<sup>29</sup>. Other groups reported that high glucose induced podocyte injury and subsequent apoptotic events might involve the Notch pathway (via Bcl-2 and p52)<sup>30</sup>, Wnt/ $\beta$ -catenin signaling<sup>31</sup>, calcineurin/NFAT2/Bax pathway<sup>32,33</sup>, or RhoA/ROCK axis<sup>34</sup>. Evidently, there is some discrepancy in the reported data, and the mechanism of TRPC6 channel activation in hyperglycemic conditions requires additional studies. Glucose can activate local RAS systems in the podocytes, leading both to increased production of Ang II by these cells and enhanced Ang II receptor expression<sup>35</sup>. Clearly, Ang II is one of the major stimuli causing calcium influx through TRPC6 channels, and there is a variety of putative pathways which could contribute to Ang II-induced podocyte injury. We have shown that Ang II causes an acute release of H<sub>2</sub>O<sub>2</sub> in the kidney<sup>36</sup>, and a compelling study by Anderson *et al.* demonstrated that Ang II-dependent activation of TRPC6

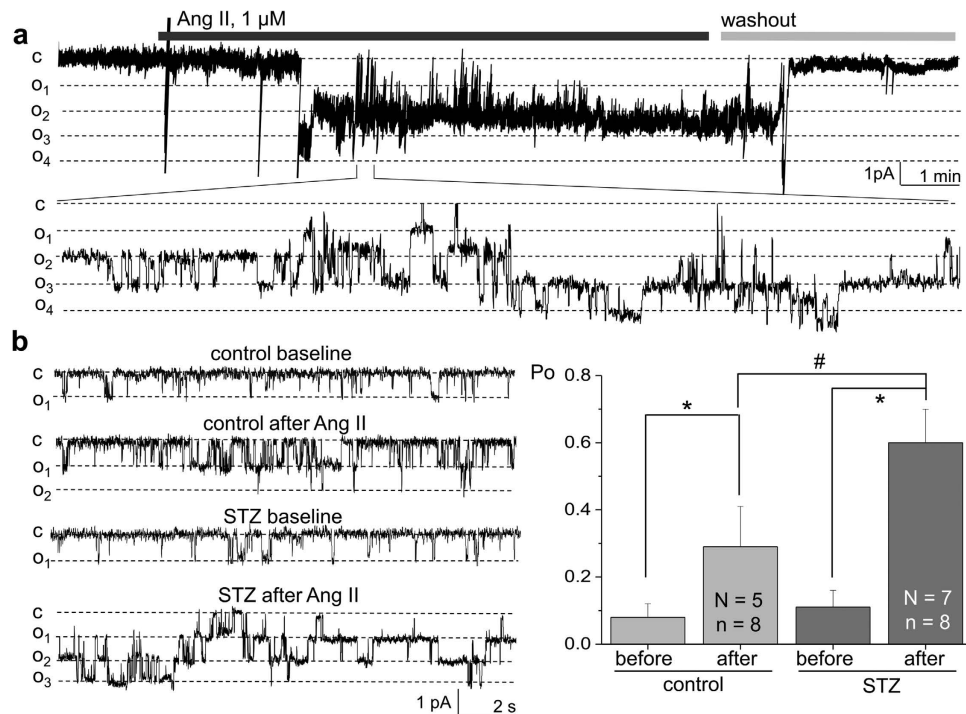


**Figure 5. Activity of TRPC6 channels in response to Ang II in type 1 diabetes.** (a) A representative patch-clamp recording showing the activation of TRPC channels in the podocytes of the control (vehicle-treated) SS rats in response to application of  $1 \mu\text{M}$  Ang II, followed by a washout of Ang II. c and  $o_i$  denote closed and open states of the channel, respectively; a full recording (upper row) and a fragment of a recording at a larger scale are shown. The recording was obtained at  $-60 \text{ mV}$ . (b) Right panel demonstrates a summary graph of the open probability ( $P_o$ ) of the TRPC channels recorded in the podocytes of the STZ-treated animals compared to control rats after acute stimulation with  $1 \mu\text{M}$  of Ang II. Representative current traces illustrating TRPC channels' activity in podocytes of diabetic rats vs. control animals (before and after application of Ang II) are shown on the left panel. N represents number of animals studied, and n is the number of analyzed patch-clamp recordings; the recordings were obtained at  $-60 \text{ mV}$ . \* and # denote statistical significance ( $P < 0.05$ ).

channels in podocytes requires generation of ROS<sup>37</sup>. These findings are critical, as diabetes development is associated with oxidative stress<sup>38</sup>, and *in vivo* administration of the ROS scavenger TEMPOL in STZ-treated rats had a renoprotective effect and ameliorated the pathological changes in glomeruli, possibly by reducing the expression of TRPC6 channels<sup>39</sup>.

A recent comprehensive study by Sonneveld *et al.*<sup>40</sup> conducted in cultured podocytes and STZ-treated Sprague Dawley rats elegantly demonstrated that TRPC6 channel expression is regulated by glucose in an Ang II-dependent manner. However, the type 1 diabetic STZ-treated Sprague-Dawley rat model is resistant to the development of DN<sup>24</sup>. The majority of recent studies on Ang II/TRPC6 interplay, although very thoroughly conducted, could have been greatly supplemented by studies carried out in an actual DN model. Here we utilized a high throughput imaging technique to monitor calcium concentration changes in the podocytes of freshly isolated glomeruli (as distinct from cultured cells), and found that Ang II – mediated calcium transient was significantly enhanced in STZ-SS rats. We have shown earlier using a mouse TRPC6 knockout model<sup>20</sup> that major calcium influx in response to Ang II in the podocytes is mediated via TRPC6 channels. Furthermore, here we report the increase in the TRPC6 channels' open probability and expression in response to Ang II in podocytes of diabetic animals. However, we do not exclude that in podocytes in diabetic condition the expression of other members of TRPC channels family could be altered as well. Furthermore, members of the TRPC family are shown to be expressed in mesangial cells<sup>41–43</sup>, and it was reported that Ang II signaling plays an important role in this type of cells<sup>44,45</sup>. Interestingly, Graham *et al.* demonstrated that abundance of TRPC6 is decreased in cultured mesangial cells treated with high glucose<sup>46,47</sup>. Furthermore, the authors showed that TRPC6 protein in glomeruli isolated from STZ-diabetic rats was decreased compared with the glomeruli from nondiabetic control rats<sup>46</sup>. These discrepancy with the findings reported here might be, for instance, contributed to the fact that Graham *et al.* used Sprague-Dawley rats in their experiments, and there is high possibility that in this model DN has not developed to a sufficient degree. In any case, additional studies are required to fully evaluate the role of TRPC channels in all types of glomeruli cells, including podocytes and mesangial cells.

Further delineating the mechanistic side of the Ang II-dependent regulation of the TRPC6 channels is of utmost importance in experimental nephrology, as it will provide functional tools to ameliorate proteinuria and prevent podocyte dysfunction in the early onset of DN. The use of numerous knockout rat models recently generated in the Dahl SS rat background expands our opportunities to study this mechanism. For instance, it is still unclear which Ang II receptor is involved in the signal transduction in the podocytes. Convincing data have been reported

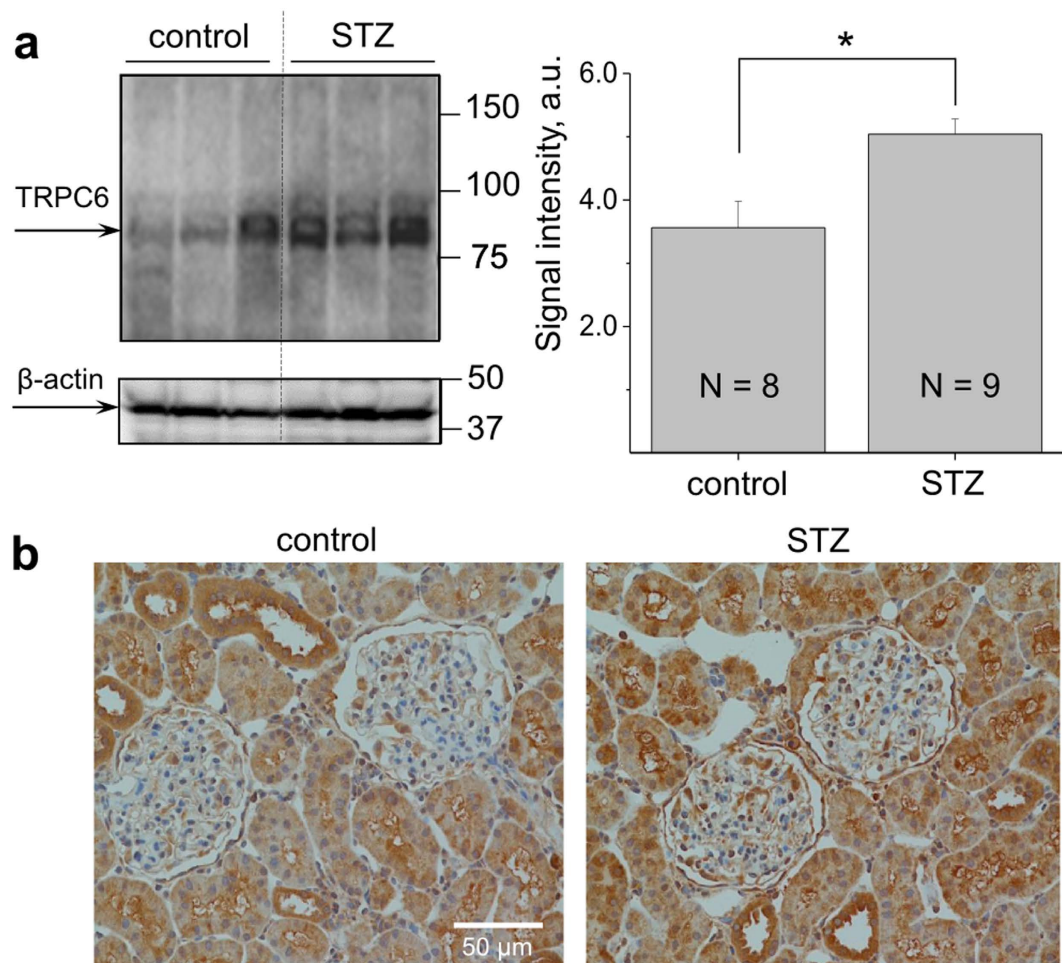


**Figure 6. Expression levels of TRPC6 channels in the cortex of STZ-treated and control rats.** (a) A representative Western blot and a summary graph for the densitometry values of the TRPC6 channel signal blotted from the cortical kidney lysates of the control and STZ-treated rats (terminal point, 11 weeks after STZ injection). Loading control for the representative blot ( $\beta$ -actin) and number of animals per group analyzed in the summary graph (N) are shown. Asterisk denotes statistical significance ( $P < 0.05$ ). (b) Images of the representative immunohistochemical stainings for TRPC6 in the control and STZ-treated rats. Magnification – 20x; scale bar is shown.

which supports the involvement of both  $AT_1R$  and  $AT_2R$  in glomeruli permeability to albumin<sup>48</sup>; both receptors are expressed in the podocytes, however the full functional relevance of this expression is yet to be revealed, particularly in disease conditions<sup>49,50</sup>.

In conclusion, we provided evidence that the effects of Ang II on calcium influx via TRPC6 in the podocytes are aggravated under the condition of type 1 DN; this finding opens up promising avenues of research to study the therapeutic modality of TRPC6 inhibition in DN or manipulating signaling pathways leading to activation of these channels.

## Methods

**Animals.** Animal use and welfare adhered to the NIH Guide for the Care and Use of Laboratory Animals following a protocol reviewed and approved by the IACUC of the Medical College of Wisconsin. 12 and 18 weeks old male Dahl Salt Sensitive rats (SS/JrHsdMcwi) were used for experiments. Food (0.4% NaCl AIN-76 diet (#113755, Dyets, Bethlehem, PA)) and water were provided *ad libitum*.

**Induction of Type 1 diabetes via a streptozotocin injection.** Experimental protocol used for type 1 diabetes induction in the Dahl SS rat was modified from Slaughter *et al.*<sup>24</sup>; a schematic illustrating the time course of the experiment is shown in Fig. 1a and Supplementary Fig. 1a (6 week long and 11 week long protocols, respectively). An intraperitoneal 75 mg/kg streptozotocin (or vehicle for control animals, 50 mM citric acid pH 4.5) injection was performed in 6 week old animals on day 0. The animals were then monitored and diabetes induction was confirmed by a blood glucose measurement (blood was obtained with a tail vein puncture) at day 5. Insulin (or sham) pellet (LinShin, Canada) was implanted *s.c.* between scapulas on day 7 in order to maintain moderate hyperglycemia (~300 mg/dL). Rats were euthanized and glomeruli were analyzed on day 42 or 77 for 6 or 11 week long protocols. Blood glucose, body weight, and 24 hour urine volume were monitored throughout the experiment.



**Kidney flush and glomeruli isolation.** At the end of the protocols, the kidneys of STZ-treated or control rats were perfused (6 ml/min) through the distal aorta with saline to clear blood from the organs, then the kidneys were collected, and glomeruli were isolated according to our published protocols<sup>20,51</sup>. Minced cortical tissue was sequentially pushed through dissociation sieves of 100 and then 140 mesh (04–881-5Z and 04–881-5 X; Thermo Fisher). The suspension was then pipetted onto a 200 mesh sieve (S4145; Sigma-Aldrich) leaving the glomeruli on the top surface. The glomeruli were then rinsed into a 15 ml tube, and used for microscopy or electrophysiology experiments<sup>26</sup>.

**Urinary nephrin ELISA assay and biochemical analysis of protein and electrolytes in plasma and urine.** Urine was collected in metabolic cages during the 6 and 11 week long experiments; urinary nephrin level was measured by a 96 well plate method with ELISA kit (Exocell, Cat #1019).  $\text{Na}^+$ ,  $\text{K}^+$ , total protein, microalbumin and creatinine levels were analyzed as described previously<sup>52</sup>.

**Western blotting.** Western blot analysis of the blood-free kidney cortex was performed as reported previously<sup>52</sup> using antibodies against an intracellular epitope of the TRPC6 ion channel (cat no ACC-017, Alomone Labs).

**Immunohistochemistry.** Isolated kidneys were fixed in 10% Formalin and routinely embedded, cut at 4  $\mu\text{m}$  slices, dried and deparaffinized for subsequent histochemistry. Hematoxylin and Eosin (H&E) staining was used to assess kidney morphology. Tissue sections were incubated with anti-TRPC6 antibodies (1:50 dilution; ACC-120, Alomone Labs). Secondary detection was performed with goat anti-rabbit biotinylated IgG (Biocare) followed by streptavidin horseradish peroxidase (Biocare) and visualized with DAB (DAKO). All slides were counterstained with a Mayer hematoxylin (DAKO), dehydrated, and mounted with permanent mounting media (Sakura).

For damage analysis, the tissue was stained with Masson's Trichrome, and individual glomeruli were evaluated using the method by Raji *et al.*<sup>53</sup> and used previously by us<sup>52</sup>. In brief, glomeruli were scored on a 0–4 scale, where score 0 is a healthy glomerulus (no sclerosis), score 1 represented a 01–25% of mesangial expansion and sclerosis (thickening of the basement membrane and/or irregular lumina of capillaries), 2 was characterized by a 26–50% of mesangial expansion and sclerosis (mild segmental hyalinosis involving 50% of the glomerular tuft), 3 glomeruli had a 51–75% of mesangial expansion and sclerosis (diffuse hyalinosis/sclerosis involving 50% of the glomerular tuft), and score 4 represented a 76–100% of glomerular mesangial expansion and sclerosis (diffuse glomerulosclerosis with total tuft obliteration)<sup>24,54</sup>. The tissues were randomized and coded before being submitted for blocking, sectioning, and staining. The code was not broken until all of the glomerular injury scoring was completed. Two independent trained observers performed the analysis of each of the slides before the actual rat ID was revealed for the final determination of group results.

**Electrophysiology.** Cover glasses with attached glomeruli were placed into a perfusion chamber and mounted on an inverted Nikon Ti-S microscope. After a high resistance seal was obtained, cell-attached recording was performed immediately in the solutions described previously<sup>20,51</sup>. Single-channel unitary current ( $i$ ) was determined from the best-fit Gaussian distribution of amplitude histograms. Activity was analyzed as  $\text{NP}_o = I/i$ , where  $I$  is the mean total current in a patch and  $i$  is unitary current at this voltage.  $P_o$  was calculated by normalizing  $\text{NP}_o$  for the total number of estimated channels ( $N$ ) in the patch. The activity of the channels was first monitored in response to the voltage steps of 10 or 20 mV in the range of  $-90$  mV to  $+60$  mV in order to estimate the channel's conductance and I-V relationship. After that, the voltage was clamped at  $-60$  mV and the channels' activity was recorded for several minutes before application of Ang II.

**Confocal laser-scanning fluorescence microscopy.** Calcium imaging was performed with laser scanning confocal microscope system Nikon A1-R. Images were collected in time series ( $xyt$ , 4 s per frame) with the Nikon imaging software. Changes in intracellular  $\text{Ca}^{2+}$  concentration were estimated from fluorescence images of Fluo-4,AM (excitation at 488 nm, emission at  $520 \pm 20$  nm). Emitted light was collected by the objective lens Plan Apo  $\times 60$  oil DIC2. The glomeruli suspension was loaded with Fluo-4,AM (5  $\mu\text{M}$ ; Invitrogen) dissolved in DMSO for approximately 30 min. Glomeruli were then mounted on poly-L-lysine covered glass in a registration chamber and washed for  $\sim 10$  min with bath solution containing (in mM): 145 NaCl, 2  $\text{CaCl}_2$ , 4.5 KCl, 2  $\text{MgCl}_2$ , 10 Hepes, pH 7.35 (adjusted with NaOH). Calcium concentration measurements were conducted as described previously<sup>20,55,56</sup>.

**Calculations and statistics.** Figure preparation and statistical analyses was carried out using MicroCal Origin software 6.0 (MicroCal Software Inc., MA, USA). Fluorescent images were processed with open source software ImageJ 1.42. All summarized data are reported as mean  $\pm$  S.E.M. Statistical difference was tested with either the Student's (two-tailed)  $t$ -test. Significance was accepted at  $P < 0.05$  or less.

## References

- Zhang, P. *et al.* Global healthcare expenditure on diabetes for 2010 and 2030. *Diabetes Res. Clin. Pract.* **87**, 293–301 (2010).
- Tervaert, T. W. *et al.* Pathologic classification of diabetic nephropathy. *J. Am. Soc. Nephrol.* **21**, 556–563 (2010).
- Pagalunan, M. E. *et al.* Podocyte loss and progressive glomerular injury in type II diabetes. *J. Clin. Invest.* **99**, 342–348 (1997).
- Wolf, G., Chen, S. & Ziyadeh, F. N. From the periphery of the glomerular capillary wall toward the center of disease: podocyte injury comes of age in diabetic nephropathy. *Diabetes* **54**, 1626–1634 (2005).
- Fogo, A. B. The targeted podocyte. *J. Clin. Invest.* **121**, 2142–2145 (2011).
- Scott, R. P. & Quaggin, S. E. The cell biology of renal filtration. *J. Cell Biol.* **209**, 199–210 (2015).
- Johnstone, D. B. & Holzman, L. B. Clinical impact of research on the podocyte slit diaphragm. *Nat. Clin. Pract. Nephrol.* **2**, 271–282 (2006).
- Lee, S. H. *et al.* Podocyte hypertrophy precedes apoptosis under experimental diabetic conditions. *Apoptosis*, **20**, 1056–1071 (2015).
- Puelles, V. G. & Bertram, J. F. Counting glomeruli and podocytes: rationale and methodologies. *Curr. Opin. Nephrol. Hypertens.*, **24**, 224–230 (2015).



10. Reiser, J. *et al.* TRPC6 is a glomerular slit diaphragm-associated channel required for normal renal function. *Nat. Genet.* **37**, 739–744 (2005).
11. Dietrich, A., Chubanov, V. & Gudermann, T. Renal TRP channels. *J. Am. Soc. Nephrol.* **21**, 736–744 (2010).
12. Winn, M. P. *et al.* A mutation in the TRPC6 cation channel causes familial focal segmental glomerulosclerosis. *Science* **308**, 1801–1804 (2005).
13. Moller, C. C. *et al.* Induction of TRPC6 channel in acquired forms of proteinuric kidney disease. *J. Am. Soc. Nephrol.* **18**, 29–36 (2007).
14. Zhang, X., Song, Z., Guo, Y. & Zhou, M. The novel role of TRPC6 in vitamin D ameliorating podocyte injury in STZ-induced diabetic rats. *Mol. Cell. Biochem.* **399**, 155–165 (2014).
15. Schlondorff, J., del Camino, D., Carrasquillo, R., Lacey, V. & Pollak, M. R. TRPC6 mutations associated with focal segmental glomerulosclerosis cause constitutive activation of NFAT-dependent transcription. *Am. J. Physiol. Cell Physiol.* **296**, C558–C569 (2009).
16. Chen, S. *et al.* Calcium entry via TRPC6 mediates albumin overload-induced endoplasmic reticulum stress and apoptosis in podocytes. *Cell Calcium* **50**, 523–529 (2011).
17. Evans, J. F., Lee, J. H. & Ragolia, L. Ang-II-induced Ca(2+) influx is mediated by the 1/4/5 subgroup of the transient receptor potential proteins in cultured aortic smooth muscle cells from diabetic Goto-Kakizaki rats. *Mol. Cell. Endocrinol.* **302**, 49–57 (2009).
18. Abkhezr, M. & Dryer, S. E. Angiotensin II and canonical transient receptor potential-6 activation stimulate release of a signal transducer and activator of transcription 3-activating factor from mouse podocytes. *Mol. Pharmacol.* **86**, 150–158 (2014).
19. Anderson, M., Kim, E. Y., Hagmann, H., Benzinger, T. & Dryer, S. E. Opposing effects of podocin on the gating of podocyte TRPC6 channels evoked by membrane stretch or diacylglycerol. *Am. J. Physiol. Cell Physiol.* **305**, C276–289 (2013).
20. Ilatovskaya, D. V. *et al.* Angiotensin II has acute effects on TRPC6 channels in podocytes of freshly isolated glomeruli. *Kidney Int.* **86**, 506–514 (2014).
21. Nijenhuis, T. *et al.* Angiotensin II contributes to podocyte injury by increasing TRPC6 expression via an NFAT-mediated positive feedback signaling pathway. *Am. J. Pathol.* **179**, 1719–1732 (2011).
22. Eckel, J. *et al.* TRPC6 enhances angiotensin II-induced albuminuria. *J. Am. Soc. Nephrol.* **22**, 526–535 (2011).
23. Zhang, H., Ding, J., Fan, Q. & Liu, S. TRPC6 up-regulation in Ang II-induced podocyte apoptosis might result from ERK activation and NF- $\kappa$ B translocation. *Exp. Biol. Med.* **234**, 1029–1036 (2009).
24. Slaughter, T. N. *et al.* Characterization of the development of renal injury in Type-1 diabetic Dahl salt-sensitive rats. *Am. J. Physiol. Regul. Integr. Comp. Physiol.* **305**, R727–734 (2013).
25. Patari, A. *et al.* Nephropathy in diabetic nephropathy of type 1 diabetes. *Diabetes* **52**, 2969–2974 (2003).
26. Ilatovskaya, D. V., Palygin, O., Levchenko, V. & Staruschenko, A. Single-channel Analysis and Calcium Imaging in the Podocytes of the Freshly Isolated Glomeruli. *J. Vis. Exp.* **e52850** (2015).
27. Krall, P. *et al.* Podocyte-specific overexpression of wild type or mutant trpc6 in mice is sufficient to cause glomerular disease. *PLoS ONE* **5**, e12859 (2010).
28. Liu, B. C. *et al.* High glucose induces podocyte apoptosis by stimulating TRPC6 via elevation of reactive oxygen species. *Biochim. Biophys. Acta* **1833**, 1434–1442 (2013).
29. Thilo, F., Lee, M., Xia, S., Zakrzewicz, A. & Tepel, M. High glucose modifies transient receptor potential canonical type 6 channels via increased oxidative stress and syndecan-4 in human podocytes. *Biochem. Biophys. Res. Commun.* **450**, 312–317 (2014).
30. Gao, F. *et al.* Notch pathway is involved in high glucose-induced apoptosis in podocytes via Bcl-2 and p53 pathways. *J. Cell. Biochem.* **114**, 1029–1038 (2013).
31. Li, Z., Xu, J., Xu, P., Liu, S. & Yang, Z. Wnt/beta-catenin signalling pathway mediates high glucose induced cell injury through activation of TRPC6 in podocytes. *Cell Prolif.* **46**, 76–85 (2013).
32. Li, R. *et al.* NFAT2 mediates high glucose-induced glomerular podocyte apoptosis through increased Bax expression. *Exp. Cell Res.* **319**, 992–1000 (2013).
33. Zhang, L. *et al.* NFAT2 inhibitor ameliorates diabetic nephropathy and podocyte injury in db/db mice. *Br. J. Pharmacol.* **170**, 426–439 (2013).
34. Yang, H. *et al.* High glucose-induced apoptosis in cultured podocytes involves TRPC6-dependent calcium entry via the RhoA/ROCK pathway. *Biochem. Biophys. Res. Commun.* **434**, 394–400 (2013).
35. Durvasula, R. V. & Shankland, S. J. Activation of a local renin angiotensin system in podocytes by glucose. *Am. J. Physiol. Renal Physiol.* **294**, F830–839 (2008).
36. Palygin, O. *et al.* Real-time electrochemical detection of ATP and H<sub>2</sub>O<sub>2</sub> release in freshly isolated kidneys. *Am. J. Physiol. Renal Physiol.* **305**, F134–F141 (2013).
37. Anderson, M., Roshanravan, H., Khine, J. & Dryer, S. E. Angiotensin II activation of TRPC6 channels in rat podocytes requires generation of reactive oxygen species. *J. Cell. Physiol.* **229**, 434–442 (2014).
38. Anil Kumar, P., Welsh, G. I., Saleem, M. A. & Menon, R. K. Molecular and cellular events mediating glomerular podocyte dysfunction and depletion in diabetes mellitus. *Front. Endocrinol. (Lausanne)* **5**, 151 (2014).
39. Luan, J. *et al.* Renal protection of *in vivo* administration of tempol in streptozotocin-induced diabetic rats. *J. Pharmacol. Sci.* **119**, 167–176 (2012).
40. Sonneveld, R. *et al.* Glucose specifically regulates TRPC6 expression in the podocyte in an AngII-dependent manner. *Am. J. Pathol.* **184**, 1715–1726 (2014).
41. He, F. *et al.* MiR-135a promotes renal fibrosis in diabetic nephropathy by regulating TRPC1. *Diabetologia* **57**, 1726–1736 (2014).
42. Meng, K. *et al.* Calcium sensing receptor modulates extracellular calcium entry and proliferation via TRPC3/6 channels in cultured human mesangial cells. *PLoS ONE* **9**, e98777 (2014).
43. Wang, Y. *et al.* Nuclear factor  $\kappa$ B mediates suppression of canonical transient receptor potential 6 expression by reactive oxygen species and protein kinase C in kidney cells. *The J. Biol. Chem.* **288**, 12852–12865 (2013).
44. Qiu, G. & Ji, Z. AngII-induced glomerular mesangial cell proliferation inhibited by losartan via changes in intracellular calcium ion concentration. *Clin. Exp. Med.* **14**, 169–176 (2014).
45. Adebisi, A., Soni, H., John, T. A. & Yang, F. Lipid rafts are required for signal transduction by angiotensin II receptor type 1 in neonatal glomerular mesangial cells. *Exp. Cell Res.* **324**, 92–104 (2014).
46. Graham, S. *et al.* Abundance of TRPC6 protein in glomerular mesangial cells is decreased by ROS and PKC in diabetes. *Am. J. Physiol. Cell Physiol.* **301**, C304–315 (2011).
47. Graham, S. *et al.* Downregulation of TRPC6 protein expression by high glucose, a possible mechanism for the impaired Ca<sup>2+</sup> signaling in glomerular mesangial cells in diabetes. *Am. J. Physiol. Renal Physiol.* **293**, F1381–1390 (2007).
48. Schiessl, I. M. & Castrop, H. Angiotensin II AT<sub>2</sub> receptor activation attenuates AT<sub>1</sub> receptor-induced increases in the glomerular filtration of albumin: a multiphoton microscopy study. *Am. J. Physiol. Renal Physiol.* **305**, F1189–1200 (2013).
49. Sharma, R., Sharma, M., Vamos, S., Savin, V. J. & Wiegmann, T. B. Both subtype 1 and 2 receptors of angiotensin II participate in regulation of intracellular calcium in glomerular epithelial cells. *J. Lab. Clin. Med.* **138**, 40–49 (2001).
50. Wang, L., Flannery, P. J. & Spurney, R. F. Characterization of angiotensin II-receptor subtypes in podocytes. *J. Lab. Clin. Med.* **142**, 313–321 (2003).
51. Ilatovskaya, D. & Staruschenko, A. Single-channel analysis of TRPC channels in the podocytes of freshly isolated glomeruli. *Methods Mol. Biol.* **998**, 355–369 (2013).

52. Pavlov, T. S. *et al.* Deficiency of renal cortical EGF increases ENaC activity and contributes to salt-sensitive hypertension. *J. Am. Soc. Nephrol.* **24**, 1053–1062 (2013).
53. Raij, L., Azar, S. & Keane, W. Mesangial immune injury, hypertension, and progressive glomerular damage in Dahl rats. *Kidney Int.* **26**, 137–143 (1984).
54. Dworkin, L. D., Feiner, H. D. & Randazzo, J. Glomerular hypertension and injury in desoxycorticosterone-salt rats on antihypertensive therapy. *Kidney Int.* **31**, 718–724 (1987).
55. Ilatovskaya, D. V., Palygin, O., Levchenko, V. & Staruschenko, A. Pharmacological characterization of the P2 receptors profile in the podocytes of the freshly isolated rat glomeruli. *Am. J. Physiol. Cell Physiol.* **305**, C1050–1059 (2013).
56. Peti-Peterdi, J. Calcium wave of tubuloglomerular feedback. *Am. J. Physiol. Renal Physiol.* **291**, F473–F480 (2006).

## Acknowledgements

This research was supported by the NHLBI R01 HL108880, R01 HL122662 (to AS) and T32 HL007852 (to AL), the American Diabetes Association grant 1-15-BS-172 (to AS), the Ben J. Lipps Research Fellowship from the American Society of Nephrology (to DVI), and the Young Investigator Grant from the National Kidney Foundation (to OP). The Authors would like to thank Colleen Lavin (Nikon Inc) for the excellent technical advice and Christine Duris (MCW) for assistance with histological staining.

## Author Contributions

Conceptualization, D.I., O.P. and A.S.; Investigation, D.I., V.L., A.L., L.S. and O.P.; Writing – original draft, D.I. and A.S.; Supervision, A.S.; All authors reviewed the manuscript.

## Additional Information

**Supplementary information** accompanies this paper at <http://www.nature.com/srep>

**Competing financial interests:** The authors declare no competing financial interests.

**How to cite this article:** Ilatovskaya, D. V. *et al.* Podocyte injury in diabetic nephropathy: implications of angiotensin II – dependent activation of TRPC channels. *Sci. Rep.* **5**, 17637; doi: 10.1038/srep17637 (2015).



This work is licensed under a Creative Commons Attribution 4.0 International License. The images or other third party material in this article are included in the article's Creative Commons license, unless indicated otherwise in the credit line; if the material is not included under the Creative Commons license, users will need to obtain permission from the license holder to reproduce the material. To view a copy of this license, visit <http://creativecommons.org/licenses/by/4.0/>